J. Chem. Sci. Vol. 128, No. 5, May 2016, pp. 815–824. © Indian Academy of Sciences.
DOI 10.1007/s12039-016-1077-1

Synthesis, crystal structure and characterization of new biologically active Cu(II) complexes with ligand derived from N-substituted sulfonamide

ADRIANA CORINA HANGAN[a], ALEXANDRU TURZA[b], ROXANA LIANA STAN[c,*], BOGDAN SEVASTRE[d], EMÖKE PÁLL[d], SÎNZIANA CETEAN[a] and LUMINIŢA SIMONA OPREAN[a]

[a]Department of Inorganic Chemistry, Faculty of Pharmacy, University of Medicine and Pharmacy, Cluj-Napoca 4000012, Romania
[b]National Institute for R&D of Isotopic and Molecular Technologies, Cluj-Napoca 400293, Romania
[c]Department of Pharmaceutical Biochemistry and Clinical Laboratory, Faculty of Pharmacy, University of Medicine and Pharmacy, Cluj-Napoca 4000012, Romania
[d]Paraclinic/Clinic Department, Faculty of Veterinary Medicine, University of Agricultural Science and Veterinary Medicine, Cluj-Napoca 400372, Romania
e-mail: acomsa6@yahoo.com; turzaalex@yahoo.com; roxanaluc@yahoo.com; bogdan.sevastre@usamvcluj.ro

MS received 20 August 2015; revised 14 March 2016; accepted 21 March 2016

Abstract. A new N-sulfonamide ligand (HL1= N-(5-(4-methoxyphenyl)-[1,3,4]–thiadiazole–2-yl)-toluene-sulfonamide) and two Cu(II) complexes, $[Cu(L1)_2(py)_2]$ (C1) and $[Cu(L2)_2(py)_2(H_2O)]$ (C2) (HL2 = N-(5-(4-methylphenyl)-[1,3,4]–thiadiazole–2-yl)-benzenesulfonamide) were synthesized. The X-ray crystal structures of the complexes were determined. In the complex C1, the Cu(II) ion is four-coordinated, forming a CuN_4 chromophore and in the complex C2, the Cu(II) ion is five-coordinated, forming a CuN_4O chromophore. The ligand acts as monodentate, coordinating the Cu(II) ion through a single $N_{thiadiazole}$ atom. The molecules from the reaction medium (pyridine and water) are also involved in the coordination of the Cu(II) ion. The complexes C1 and C2 are square-planar and a slightly distorted square pyramidal, respectively. The compounds were characterized by FT-IR, electronic, EPR spectroscopic and magnetic methods. The nuclease binding activity studies of the synthesized complexes confirm their capacity to cleave the DNA molecule. The cytotoxicity studies were carried out on melanoma cell line WM35 which confirm that both compounds inhibit the growth of these cells. They have a higher activity compared to a platinum drug, carboplatin.

Keywords. Sulfonamide; Cu(II) complexes; crystal structure; oxidative DNA cleavage; cytotoxic activity.

1. Introduction

The continuous demand for new anti-cancer drugs has stimulated chemotherapeutic research based on the use of essential metallic elements since potential drugs developed in this way may be less toxic and more prone to exhibit antiproliferative activity against tumors.[1–4] A great number of chemical substances are known to possess *in vitro* biocatalytic activity, emulating different enzymatic processes. Among these chemicals, copper-coordinated compounds have shown superoxide dismutase and/or nuclease activities, depending on the type of ligand present. Although many studies were made, the metal containing drugs are relatively rare. A platinum containing compound, cisplatin is one of the most effective antitumor drugs. Unfortunately, cisplatin therapy has severe side effects, which limit the clinical use.[5] Therefore, finding a new potential metal based less toxic anticancer drug is a very active area of research.[6] In this context, Cu(II) and its complexes play an important role as suitable compounds for antiproliferative tests.[1–4] Cu(II) complexes have justified interest because they have biologically accessible redox potentials and significant affinity for the nuclear bases.[7] Cu(II) ion seems to play a critical role in angiogenesis, a key event in tumor promotion and progression.[8] Some Cu(II) complexes are able to interact with DNA by electrostatic and partial insertion of pyridyl rings between the base stacks of double-stranded DNA, thus showing cytotoxic effects on several human carcinoma

*For correspondence

cell lines.[9] Further evidences show that reactive oxygen species play an important role in cell apoptosis induced by Cu(II) complexes,[10] through the intrinsic pathway accompanied by the regulation of p53, Bcl-2 family proteins.[11,12] The toxicity of Cu(II) complexes seems to be lower than classic cancer therapy.[13]

For the past several years, our group has worked on the synthesis of Cu(II) complexes with N-substituted sulphonamides in order to obtain new antitumor agents. These complexes are especially attractive as anticancer agents because several substituted sulfonamides have been found to arrest the cell cycle, causing apoptosis in the M phase.[14] In this context, we have described the nuclease activity of several copper-sulfonamide complexes.[15–17]

In this paper we report the synthesis, the physicochemical characterization of two new Cu(II) complexes with N-substituted sulfonamides and we demonstrate their antitumor activity.

2. Experimental

2.1 *Materials and physical measurements*

Copper sulfate pentahydrate, methanol, toluenesulfonylchloride, 2-amino-5-(4-methoxylphenyl)-[1,3,4]–thiadiazole and pyridine were purchased from Fluka and Merck chemical companies and were used without further purification.

Elemental analyses (C, N, H, S) were performed with Vario EL analyser. IR spectra were recorded with a Jasco FT-IR-4100 spectrophotometer using diffuse reflectance of incident radiation focused on a sample, in the 4000−450 cm^{-1} range. All melting points were determined in open capillaries with an Electrothermal IA 9100 apparatus and were uncorrected. ^{1}H NMR spectrum of the ligand was recorded at room temperature using DMSO-d6 as solvent in 5 mm tubes on Bruker AM 300 NMR spectrometer equipped with a dual, ^{1}H (multinuclear) head operating at 300 MHz for protons. Fast ion bombardment (FAB) mass spectrum of the ligand was obtained on a VG Autospec spectrometer in m-nitrobenzene as a solvent. Diffuse reflectance spectra and UV-Vis spectra of the complexes were carried out on a Jasco V-550 spectrophotometer. Magnetic susceptibility was measured at room temperature with the Faraday MSB-MKI balance. $Hg[Co(NCS)_4]$ was used as susceptibility standard. Electronic paramagnetic resonance (EPR) spectrum was recorded at room temperature with a Bruker ELEXSYS spectrometer operating at the X-band frequency.

2.2 *Synthesis of the ligands N-(5-(4-methoxyphenyl)-[1,3,4]–thiadiazole–2-yl)-toluenesulfonamide (**HL1**) and N-(5-(4-methylphenyl)-[1,3,4]–thiadiazole–2-yl)-benzenesulfonamide (**HL2**)*

A solution containing 2-amino-5-(4-methoxyphenyl)-[1,3,4]-thiadiazole (1 mmol) and toluenesulfonylchloride (0.9 mmol) in 15 mL of pyridine was heated at reflux for 1 h, at 60°C. The mixture was added to 50 mL of cold water and stirred for several minutes. The resulting solid was recrystallized from ethanol. (Yield 90%); M.p. 235-236°C, Anal. Calcd (%) for $C_{16}H_{15}N_3S_2O_3$ (MW = 361 g · mol^{-1}) C, 53.18; H, 4.15; N, 11.63; S, 17.72. Found (%): C, 53.47; H, 4.26; N, 11.94; S, 17.98. IR (KBr) ν_{max} /cm^{-1}: 3258 (ν(N-H)), 1548 (ν(C=C) aromatic), 1554 (ν(thiadiazole)), 1318 (ν_{asym} (S=O)), 1152 (ν_{sym} (S=O)); 905 (ν(S–N)). ^{1}H-NMR (DMSO-d6), δ / ppm, (J Hz): 2.37-2.36 (6H, s, H-16, H-7), 7.38-7.34 4H, d, J=7.8 Hz, H-6, H-2, H-11, H-15), 7.73-7.71 (4H, d, J=7.8 Hz, H-5, H-3, H-12, H-14), 8.52 (1H, s, H (N3)); MS m/z : 362 [M+H$^+$].

The synthesis, structure and properties of the ligand **HL2** have been reported.[18]

2.3 *Synthesis of the complexes [Cu(N-(5-(4-methoxyphenyl)-[1,3,4]-thiadiazole-2-yl) toluenesulfonamidate)$_2$ (py)$_2$] **(C1)** and [Cu(N-(5-(4-methylphenyl)-[1,3,4]-thiadiazole-2-yl) benzenesulfonamidate)$_2$(py)$_2$(H_2O)] **(C2)***

A solution of $CuSO_4 \cdot 5H_2O$ (4 mmol) in 20 mL of pyridine: H_2O [v : v = 1 : 1] was added dropwise, under continuous stirring to a solution of **HL1** or **HL2** ligand (1 mmol) dissolved in 25 mL pyridine : H_2O [v: v = 2 : 3]. The resulting solution was stirred at room temperature for two hours and left to stand at room temperature. After one and two months of slow evaporation of the solvent, respectively, brown (**C1**) and green crystals (**C2**) suitable for X-ray diffraction were obtained.

Anal. Calcd (%) for **(C1)** $C_{42}H_{38}CuN_8S_4O_6$ (MW = 942.32 g · mol^{-1}): C, 53.50; H, 4.03; N, 11.88; S, 13.58%. Found (%) C, 53.84; H, 4.22; N, 12.09; S, 13.82%. IR (KBr) ν_{max} /cm^{-1}: 1495 (ν(thiadiazole)); 1292 (ν_{asym} (S=O)), 1130 (ν_{sym}(S=O)), 932 (ν(S–N)). UV/Vis (solid) λ_{max}/nm: 318 ($\pi \rightarrow \pi^*$), 412(LMCT), 593 (d-d). 625 (d-d) ($\varepsilon = 100$ $cm^{-1}M^{-1}$) (Yield ca. 58%).

Anal. Calcd for **(C2)** $C_{40}H_{35}CuN_8S_4O_5$ (MW = 899.32 g · mol^{-1}): C, 53.37; H, 3.89; N, 12.45; S, 14.23%. Found C, 53.20; H, 3.76; N, 12.31; S, 14.35%. IR (KBr) ν_{max} /cm^{-1}: 1468(ν(thiadiazole)); 1302 (ν_{asym} (S=O)), 1134 (ν_{sym} (S=O)), 930 (ν(S–N)). UV/Vis

(solid) λ_{max}/nm: 314 ($\pi \rightarrow \pi^*$), 405 (LMCT), 589 (d-d). 605 (d-d) ($\varepsilon = 70\ cm^{-1}M^{-1}$) (Yield ca. 67%).

2.4 *X-ray crystallography*

A brown crystal of the complex (**C1**) and a green crystal of the complex (**C2**) was mounted on a glass fiber and used for data collection. Crystal data were collected at 293(2) K using a dual microsourse SuperNova Diffractometer and Cu K_α radiation ($\lambda = 1.5418$Å).

Using Olex 2,[19] the structure was solved with the Superflip[20] structure solution program using Charge Flipping and refined with the ShelXL[21] refinement package using Least Squares minimisation. A summary of the crystal data, experimental details and refinement results are listed in table 1.

2.5 *Biological assays*

2.5a *DNA cleavage*: Reactions were performed by mixing 7 μL of cacodylate buffer 0.1 M, pH 6 (cacodylic acid/sodium cacodylate), 6 μL of the complex solution (final concentrations: 3, 6, 9, 12 and 15 μM), 1 μL of pUC18 DNA solution (0.25 μg/μL, 750 μM in base pairs), and 6 μL of activating agent solution (H_2O_2/ascorbic acid) in a threefold molar excess relative to the concentration of the complex. The resulting solutions were incubated for 1 h at 37°C, after which a quench buffer solution (3 μL) consisting of bromophenol blue (0.25%), xylene cyanol (0.25%) and glycerol (30%) was added. The solution was then subjected to electrophoresis on 0.8% agarose gel in 0.5×TBE buffer (0.045 M Tris, 0.045 M boric acid, and 1 mM EDTA) containing 5μL/100 mL of a solution of ethidium bromide (10 mg/mL) at 100 V for 2 h. The bands were photographed on a capturing system (Gelprinter Plus TDI).

To test for the presence of reactive oxygen species (ROS) generated during strand scission and for possible complex-DNA interaction sites, various reactive oxygen intermediate scavengers and groove binders were added to the reaction mixtures. The scavengers used were 2,2,6,6-tetramethyl-4-piperidone (0.5 M), dimethylsulfoxide (DMSO) 14 M, *t*-butyl alcohol (10.5 M), sodium azide (NaN_3) (400 mM), superoxide dismutase (SOD) (15 units). In addition, a chelating agent of copper(I), neocuproine (36 μM), along with the groove binder distamycin (80 μM) were also assayed. Samples were treated as described above.

2.5b *Cell culture*: The assessment of antiproliferative effect was performed on WM35, a human radial growth phase melanoma cell line. WM35 cells were maintained in RPMI medium (Sigma-Aldrich), supplemented with 10% fetal calf serum (FCS, Hyclone), 1% antibiotic/antimycotic (Gibco, Invitrogen), 2 mM glutamine (Gibco, Invitrogen). The cultures were maintained in a humidified atmosphere with 5% CO_2 at 37°C.

Table 1. Crystal and refinement data for complexes **C1** and **C2**.

Empirical formula	$C_{21}H_{19}Cu_{0.5}N_4O_3S_2$	$C_{40}H_{35}CuN_8S_4O_5$
Formula weight	471.32	899.32
Temperature	293(2) K	293(2) K
Crystal system	Triclinic	Monoclinic
Space group	P-1	C c
Unit cell dimensions	a = 7.9179(5)Å α = 112.068(6)°	a = 15.0977(3) Å α = 90°
	b = 12.2586(7)Å β =94.619(5)°	b = 21.7903(4) Å β = 103.3750(17)°
	c = 12.7761(8)Å γ = 108.829(6)°	c = 13.1399(2) Å γ = 90°
Volume	1058.56(12) A^3	4205.56(8) A^3
Z	2	4
Calculated density	1.482 Mg/m^3	1.468 Mg/m^3
Absorption coefficient	3.066 mm^{-1}	3.049 mm^{-1}
F(000)	489	1928
Crystal size	0.25 × 0.21 × 0.15 mm^3	0.37 × 0.14 × 0.07 mm^3
θ range for data collection	7.68 to 58.14°	3.46 to 74.78°
Limiting indices	$-9 \leq h \leq 9, -15 \leq k \leq 14, -15 \leq l \leq 15$	$-14 \leq h \leq 18, -26 \leq k \leq 22, -16 \leq l \leq 11$
Collected refl.	15029	8243
Independent reflections	4083 [R(int) = 0.0299]	3998 [R_{int} = 0.0575]
Data/restraints/parameters	4083/0/279	5127 / 6 /552
Goodness-of-fit on F^2	1.049	1.019
Final R indices [I>2σ(I)]	R_1 = 0.0425, wR_2 = 0.1154	R1 = 0.0339, wR2 = 0.0868
R indices (all data)	R_1 = 0.0499, wR_2 = 0.1245	R1 = 0.0360, wR2 = 0.0846
Min./max. Res (e^- $Å^{-3}$)	0.39/−0.49	0.183/−0.191

2.5c *Cell toxicity assay*: The cell cytotoxicity assay was performed using the MTT test, as specified by the manufacturer. The cells were seeded at a density of 10^5 /well in ELISA 96-well micro titration flat bottom plates and allowed to accommodate for 24 h in normal growth conditions. The cultures were then exposed to complexes **C1** and **C2** in increasing concentrations, ranging from 10 to 100 μM, for 24 h. Each experiment was carried out in triplicate. Cell cultures treated only with medium were used as controls. After 24 h, the cells treated with complex **C1** and **C2,** and their control counterpart were incubated for 2 h with 200 μL of MTT. The MTT assay involves the conversion of the water soluble MTT (3-(4,5-dimethylthiazol-2-yl)-2,5-diphenyltetrazolium bromide) to an insoluble formazan. The formazan was solubilized with 200 μL DMSO and the absorbance of each sample was read at 490 nm using an ELISA microplate reader.

The IC_{50} values representing the complexes concentration required to inhibit 50% of cell proliferation were calculated from the dose response curve using PROAST 38.9 Software.

2.5d *Statistics*: All data are reported as the mean ± SEM. A minimum of three replicates were performed for each method used. Statistical analysis where performed using two-way analysis of variance (two-way ANOVA) and Bonferoni's test was used as a post hoc analysis. P – values <0.05 were considered significant. Statistical values and figures were obtained using GraphPad Prism version 5.0 for Windows, GraphPad Software, San Diego, California USA.

3. Results and Discussion

3.1 *Crystal structure of [Cu(L1)$_2$(py)$_2$] (**C1**) and [Cu(L2)$_2$(py)$_2$(H$_2$O)] (**C2**)*

A triclinic group P-1 and a monoclinic group Cc for **C1** and **C2**, respectively, were determined from single-crystal data of the complexes by X-ray crystallography. Relevant bond distances and angles for the two complexes are collected in table 2.

The molecular structure and crystallographic numbering scheme for complex **C1** are illustrated in figure 1 and for complex **C2** in figure 2.

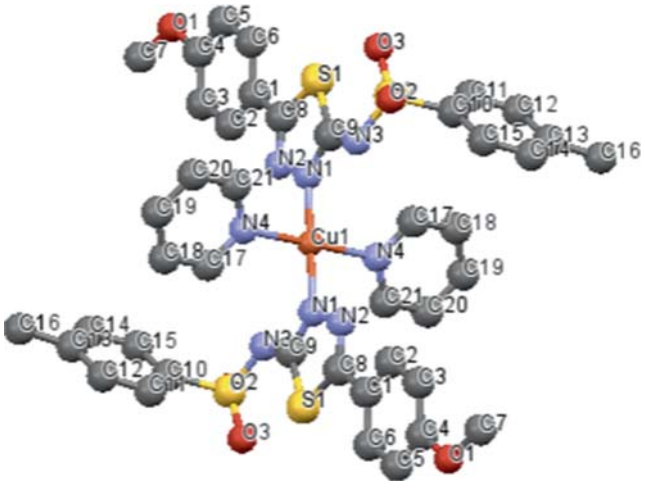

Figure 1. Molecular structure of the complex [Cu(L1)$_2$ (py)$_2$], **C1**.

Table 2. Selected bond lengths (Å), angles (°) and torsion angles for C1 and C2.

Parameters			
C1		C2	
Bond distances		*Bond distances*	
Cu1–N1	1.961 (19)	Cu1–N1	2.025 (3)
Cu1–N4	2.064 (2)	Cu1–N2	2.023 (3)
		Cu1–N3	2.026 (3)
		Cu1–N4	2.004 (3)
		Cu1–O	2.316 (3)
Bond anges		*Bond angles*	
N4'–Cu1–N4	180	N1–Cu1–N2	166.4 (1)
N1–Cu1–N4	89.52(8)	N1–Cu1–N6	91.1 (1)
N1'–Cu1–N4	90.48(8)	N1–Cu1–N4	88.6 (1)
N1'–Cu1–N4'	89.52(8)	N2–Cu1–N6	88.2 (1)
N1–Cu1–N4'	90.48(8)	N2–Cu1–N4	91.2 (1)
N1– Cu1–N1'	180	N6–Cu1–N4	176.3 (1)
		N1– Cu1–O	96.3 (1)
		N2– Cu1–O	97.3 (1)
		N6– Cu1–O	90.5 (1)
		N4–Cu1–O	93.2 (1)

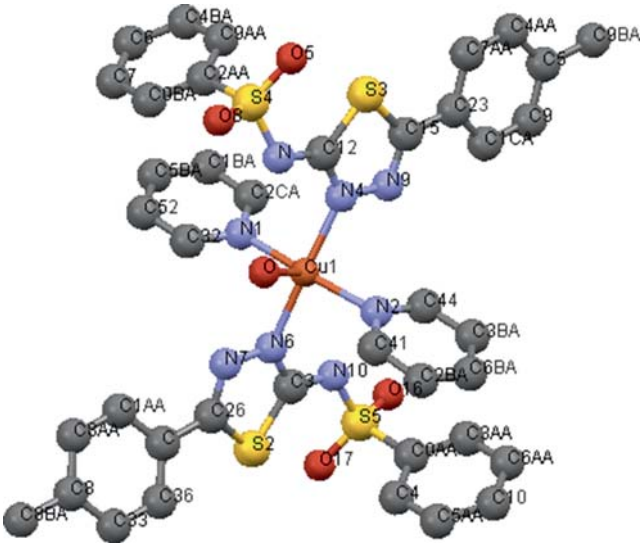

Figure 2. Molecular structure of the complex $[Cu(L2)_2(py)_2(H_2O)]$, **C2**.

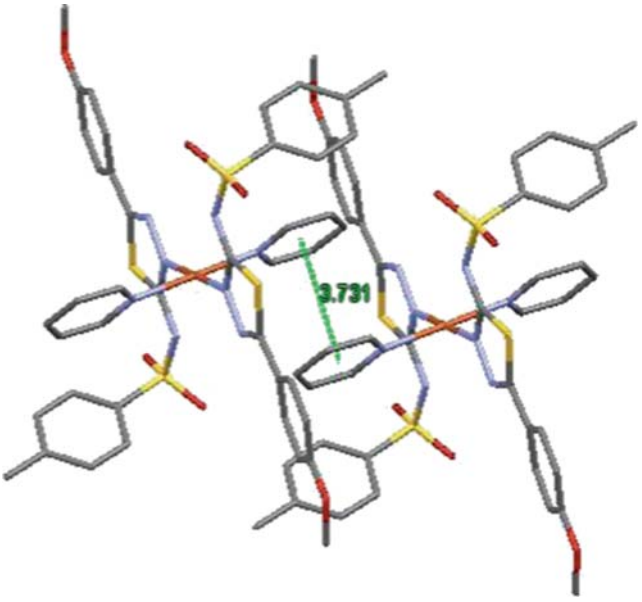

Figure 3. Crystal packing of complex $[Cu(L1)_2(py)_2]$, **C1** showing the pyridyl-pyridyl stacking interactions.

The crystal structure for the complex **C1** shows that the Cu(II) ion is four-coordinated and the cromophore-type is CuN_4. The Cu(II) ion is bound centrosymmetrically by two deprotonated ligands and two pyridine molecules in a square-planar environment. Each ligand coordinates the metal ion through the one $N_{thiadiazole}$ atom, with mean Cu1–N1 bond distances of 1.961(19) Å. The sulfonamide ligand (**HL1**) coordinates the Cu(II) ion upon the deprotonation of the –NH-SO_2- moiety. The two pyridine molecules also participate at the Cu(II) coordination by two nitrogen atoms $N_{pyridine}$ (Cu1-N4 2.064(2) Å). The N-Cu-N angles that describe the geometry of coordination range from 89.52(8)° to 90.48(8)°. The diagonal angles N4-Cu1-N4' and N1-Cu1-N1' are 180°. The Cu(II) ion is in the plane formed by the four N atoms; the dihedral angle between the planes Cu1-N1-N4 and Cu1-N1'-N4' is equal to 0° which confirms the square-planar arrangement of the CuN_4 chromophore. The distances between the Cu(II) ion and the four nitrogen atoms and the angles that describe the geometry of the complex **C1** molecule are similar to those reported in literature for copper complexes with the related sulfathiadiazole ligand.[22–24] The crystal structure of complex **C1** consists of monomer units linked by stacking interactions between the aromatic rings of pyridine molecules (mean distance between rings is 3.731(4) Å) (figure 3).

In complex **C2**, the coordination geometry of the metal ion is slightly distorted square pyramidal. The values of the distortion parameter, $\tau = 0.165$, and that of the tetragonal distortion index of the complex, $T5 = 0.87$, are indicative of a distorted square pyramidal stereochemistry.[25] The equatorial bonds are shorter, ranging from 2.004(3) Å to 2.026(3) Å, in a N4 equatorial plane, formed by two nitrogen atoms belonging to the deprotonated sulfonamide $N_{thiadiazole}$ and two nitrogen atoms of the pyridine molecules (co-ligand $N_{pyridine}$). The axial position is defined by the longest bond, formed with the oxygen atom of the one water molecule [2.316(3) Å]. It is noteworthy that the coordination of Cu(II) ion takes place through the $N_{thiadiazole}$ atom instead through the deprotonated $N_{sulfonamido}$ atom. This is a consequence of the charge delocalization between the sulfonamido and the thiadiazole ring. The sulfonamidate ligand (L^-) acts as monodentate as it coordinates through a nitrogen atom of the thiadiazole heterocycle.

The extent of the distortion of square pyramid is also reflected in the angles inside the coordination polyhedron. The angles formed by the atoms in *trans* positions slightly deviate from 180° [N1-Cu1-N2 166.4(1)°, N6-Cu1-N4 176.3(1)°], while the angles formed by the atoms in *cis* positions fall within the range of 88.2(1)°-96.3(1)°.

The deviations of N1, N2, N4 and N6 atoms from the mean plane are -0.087 Å, 0.088 Å, -0.089 Å and 0.088 Å, respectively, and the Cu(II) ion is displaced by 0.152 Å above the plane.

$\pi - \pi$ intermolecular interactions between the pyridine and benzene ring in the same molecule of complex and the pyridine molecules and toluene ring in adjacent molecules contribute to the stabilization of the $[Cu(L2)_2(py)_2(H_2O)]$ complex (figures 4a and b).

Complex **C2** is stabilized by intramolecular strong and weak hydrogen bonds,[26] implicating hydrogen

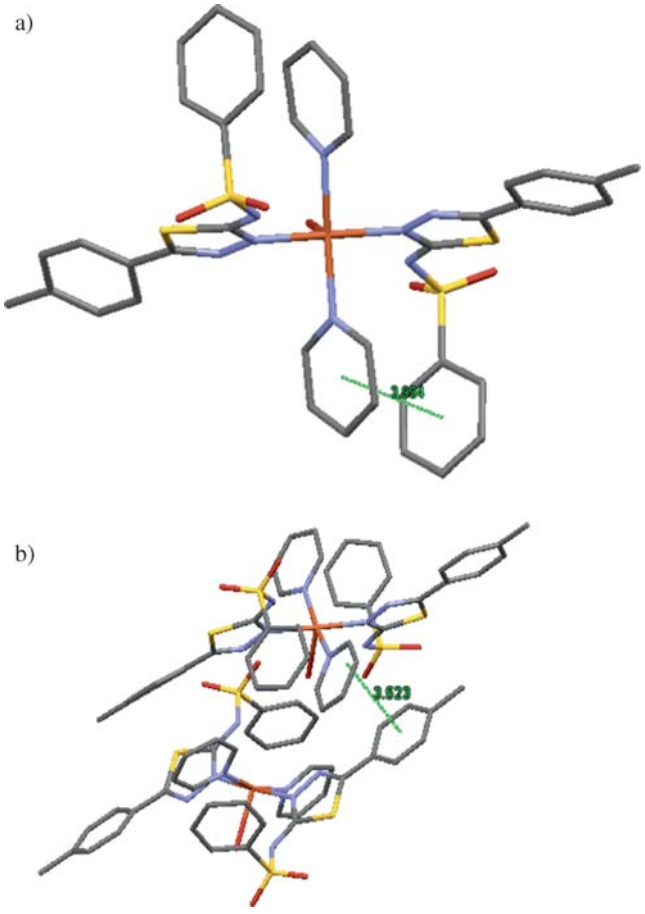

Figure 4. (**a**) Intramolecular pyridyl-phenyl π-π interactions in complex **C2**. (**b**). Intermolecular pyridyl-methylphenyl π-π interactions in complex **C2**.

atoms from the water molecule, $N_{sulfonamido}$ and $N_{thiadiazole}$ atoms, hydrogen atoms from the benzene ring and the oxygen atoms belonging to the sulfonamide groups. The geometric parameters defining the hydrogen bonds are collected in table 3.

3.2 *Spectroscopic and magnetic properties*

An important aspect to be noted on the IR spectra of the synthesized complexes is the disappearance of the band assigned to the N-H stretching vibration, indicating the deprotonation of the sulfonamides upon coordination. The proton loss induces a weak conjugation effect between the N, S and O atoms in the sulfonamide group. As a consequence of the involvement of the sulfonamide moiety in coordinating the metal center, the bands assigned to $\nu_{asym}(SO_2)$, $\nu_{sym}(SO_2)$ and ν(S-N) appear shifted to lower or higher frequencies in the IR spectra of the complexes. The bands attributed to the stretching vibrations of the thiadiazole ring, (ν(N-N) and ν(C=N)) appear shifted towards lower frequencies, as proof of the Cu(II) coordination through the $N_{thiadiazole}$ atom.

The IR spectra of complexes **C1** and **C2** show a very similar pattern. The most remarkable difference occurs in the band corresponding to the stretching vibration of the thiadiazole ring, which is shifted from 1554 cm^{-1} **(HL1)** and 1542 cm^{-1} **(HL2)** in the free ligands to 1495 cm^{-1} **(C1)** and 1468 cm^{-1} **(C2)**. The bands corresponding to $\nu_{asym}(SO_2)$ appear at 1292 and 1302 cm^{-1}, respectively, are significantly shifted towards lower frequencies with respect to the uncoordinated sulfonamide. The sharp, high intensity bands at 1130 and 1134 cm^{-1} are attributed to $\nu_{sym}(SO_2)$. The third element related to the sulfonamide moiety, the bands corresponding to the S-N bond, are identified at 932 and 930 cm^{-1}, respectively slightly shifted towards higher frequencies.

Infrared bands related to ligand and pyridine molecules are present in the spectra of the obtained crystals which prove the presence of the raw materials in the final structure as described in XRD analysis.

Literature report[27] indicates that the bands corresponding to the uncoordinated pyridine molecules appear at 3083, 3055, 3030 cm^{-1} (q(C−H)), 1581, 1573, 1481, 1437 (Q(C−C), β(CCH)), 1292, 1226 cm^{-1} (β(NCH)), 1216, 1145, 1081, 1067 cm^{-1} (β(CCH)), 991 cm^{-1} (Q (N−C)), 973, 940, 883, 748 (χ(N−C)), 704 cm^{-1} (ρ (C−H)), 653 cm^{-1} (γ(NCC)) and 604 cm^{-1} (γ(NCC)).

Thus, in the spectra of complexes bands related to pyridine only exist and they appear at the same wavenumber ∼995 and ∼1073 cm^{-1}, but at the same time, there are bands with different spectral position compared to the spectrum of the initial compound, which are situated at 1047, 1449 1492 cm^{-1}. The shift of the bands may be assigned to ν(C−C) in pyridine

Table 3. Hydrogen bonds for complex **C2**.

D-H...A	d(D-H) (Å)	d(H...A) (Å)	d(D...A) (Å)	<(DHA) (°)
O-HA ....N8 (strong)	0.871	2.004	2.775	146.96
O-HB....N7(weak)	0.871	2.371	2.944	123.63
C4-H4...O17(weak)	0.951	2.712	3.008	98.76
C3AA-H3AA...O16(weak)	0.950	2.535	2.907	103.51
C9AA-H9AA...O5(weak)	0.951	2.593	2.942	102.06
C2AA-H2AA....O8(weak)	0.950	2.653	2.976	100.50

from 1035, 1038, 1485 cm^{-1}, indicating the influence of the external environment on the pyridine ring.

The bands related to the ligand in the spectra of complexes changed their spectral positions because of the new environment. For instance, the bands at 1275, 1298, 1305 cm^{-1} in complex **C2** are shifted to lower wave numbers.

The other bands can be attributed to pyridine, as they sometimes overlap the frequencies corresponding to moieties of the ligand. The patterns of the IR spectra are similar to those observed for other Cu(II) complexes with N-substituted sulfonamides.[28–30]

The electronic spectra of the solid of both complexes display a band at 412 nm **C1** and 405 nm **C2**, which are assigned to a LMCT transition. The complex **C1** exhibits a d−d band at 593 nm and the complex **C2** shows a d−d band at 589 nm. The patterns, characteristic for a square-planar and distorted square-pyramidal geometry, respectively, agree well with the crystallographic data.[31]

The polycrystalline X-band EPR spectra indicate that complex **C1** is rhomboidal and the complex **C2** is axial. The EPR parameters, obtained by simulation are $g_x = 2.035$, $g_y = 2.075$, $g_z = 2.140$ and $A_{\parallel} = 190 \times 10^{-4}$ cm^{-1} for complex **C1;** $g_{\parallel} = 2.31$, $g_{\perp} = 2.076$ and $A_{\parallel} = 154 \times 10^{-4}$ cm^{-1} for complex **C2**.[32] According to the Bertini classification, the value of $A_{\parallel}$ for complex C**1** and C**2** can be correlated with the geometry of the complex.[33] Thus, A values between 160 and 200 $\times$ 10^{-4} cm^{-1} correspond to a square-planar geometry and values between 130 and 160 $\times$ 10^{-4} cm^{-1} correspond to a square pyramidal or distorted trigonal bipyramidal geometry. In good agreement with the regular square-planar polyhedron for complex **C1,** its g_z value is the lowest.[23,30,34]

The room temperature the magnetic moments of complex **C1** ($\mu_{eff} = 1.74$ BM) and complex **C2** ($\mu_{eff} = 1.85$ BM) are consistent with the presence of a single unpaired electron.

3.3 *DNA cleavage*

The activity of the complexes as chemical nucleases was studied using supercoiled pUC18 DNA in DMF: cacodylate buffer (0.1M, pH 6.0) at a molar proportion (1:39) in the presence of H_2O_2/ascorbic acid, 3-fold excess relative to the complex concentration. The efficiency of the complexes was compared with that of both copper sulfate and Cu(II) complex of o-phenanthroline $Cu(phen)_2]^{2+}$ under the same reaction conditions. The results, see figure 5 show that both complexes **C1** and **C2** exhibit high nuclease activity and are more effective at higher concentrations.

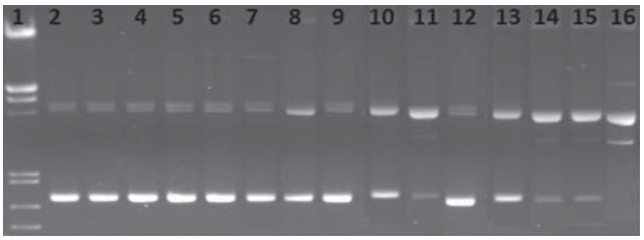

Figure 5. Electroferogram in agarose gel of the pUC18 plasmid treated with $CuSO_4$, the **C1** and **C2** complexes and copper(II) complex of o-phenathroline $[Cu(phen)_2]^{2+}$. Lane 1. base marker; 2. pUC18 control; 3. pUC18 control + reducing agents; 4. 6 μM $CuSO_4$+ reducing agents; 5. 12 μM $CuSO_4$+ reducing agents; 6. 18 μM $CuSO_4$+ reducing agents; 7. 24 μM $CuSO_4$+ reducing agents; 8. 6 μM complex C1+ reducing agents ; 9. 12 μM complex C1+ reducing agents; 10. 18 μM complex C1+ reducing agents; 11. 24 μM complex C1+ reducing agents; 12. 6 μM complex C2 + reducing agents; 13. 12 μM complex C2+ reducing agents; 14. 18 μM complex C2+ reducing agents; 15. 24 μM complex C2+ reducing agents; 16. 24 μM $[Cu(phen)_2]^{2+}$+ reducing agents.

The complexes at 18 μM (figure 5, lanes 10 and 14) produced a partial conversion of closed circular conformation DNA into its supercoiled form. At 24 μM, both compounds induce degradation of DNA molecule of the supercoiled form to open circular DNA (figure 5, lanes 11 and 15). Under the same conditions, $CuSO_4$ exhibited less nucleolytic activity than either compound (figure 5, lanes 4-7). The eletroferogram shows that the complex C2 has a superior nuclease activity. As for the $Cu(phen)_2]^{2+}$ complex, which is a well-known and very efficient chemical nuclease, we found that at a dose of 24 μM, the two complexes **C1** and **C2** are less active than $[Cu(phen)_2]^{2+}$.

The nuclease activity of the complexes **C1** and **C2** was studied in the presence of certain inhibiting agents: DMSO, t-butyl alcohol, distamycin, sodium azide, 2,2,6,6-tetramethyl-4-piperidone, superoxide dismutase and neocuproine, to determine the ROS involved in the degradation process of the DNA molecule. We chose a concentration of 24 μM for the complexes and a concentration 30 times higher for the reducing agents ascorbic acid/H_2O_2. The incubation period of the samples was of one hour, at 37°C. The resulting electroferograms are presented in figure 6.

The results of the electroferogram show that in the control sample with reducing agents (lane 2), only helicoidal DNA is present, as we expected, as they only contain the pUC18 plasmid in cacodilate/DMF buffer. Lane 3 corresponds to the complexes without inhibiting agents. The complexes degrade DNA to its linear form. By adding DMSO and t-butyl alcohol to the complexes samples (lanes 4 and 5), we can notice that its

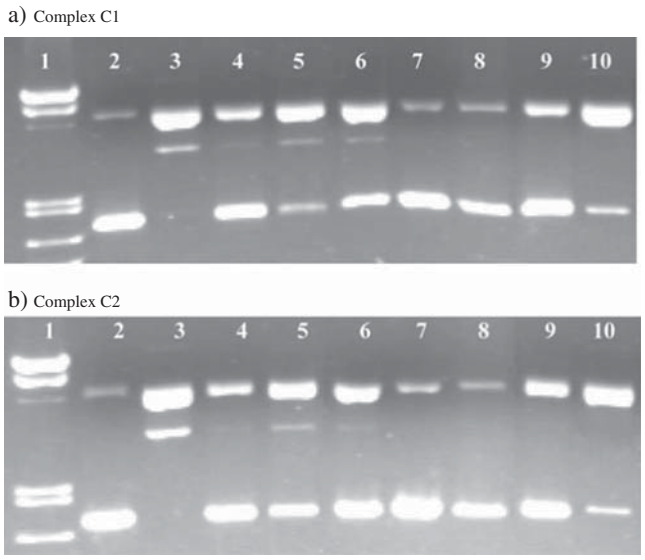

Figure 6. Electroferogram in agarose gel of the pUC18 plasmid treated with the complexes **C1** and **C2** and various inhibiting agents. Lanes: 1. base marker; 2. control; 3. complex (**C1** or **C2**) 24 μM without inhibitors+ reducing agents; 4. complex + DMSO+ reducing agents; 5. complex + t-butyl alcohol+ reducing agents; 6. complex + distamycin+ reducing agents; 7. complex + NaN_3+ reducing agents ; 8. complex + 2,2,6,6-tetramethylpiperidone+ reducing agents; 9. complex + SOD+ reducing agents; 10. complex 30 μM + neocuproine+ reducing agents.

nuclease activity is inhibited, which proves the fact that the hydroxyl radicals OH· participate in the destruction of the DNA molecule. These radicals serve as the reactive species that are directly responsible for starting the cleavage reaction. The significant decrease in the cleavage capacity of the complexes in the presence of minor groove binder distamycin (lane 6) indicates a minor groove interaction. Sodium azide and 2,2,6,6-tetramethyl-4-piperidone (lanes 7 and 8) also inhibit DNA cleavage by the compounds, which indicates the participation of $^1O_2$ or singlet-oxygen-like entities in the reaction. In the presence of SOD, the activity of the complex decreases because SOD can capture and destroy the superoxide radical ions $O_2^{\cdot-}$, produced during the reaction mechanism of the complex in the presence of reducing agents and which participate in the degradation of the DNA molecule. One of the steps in the destruction mechanism of nucleic acid is the reduction of the Cu(II) ion to Cu(I). This fact is confirmed by the decrease of the nuclease activity of the complex when using as inhibitor neocuproine (lane 10). By adding neocuproine, a stable complex of Cu(I) is formed (Cu(I)-neocuproine), thus inhibiting the subsequent reactions of the degradation mechanism of the DNA molecule. In the presence of this inhibitor, DNA is degraded only to its circular form, which coexists with the helicoidal form.

In summary, the above results indicate that the cleavage reaction involves various reactive oxygen species, hydroxyl radicals, singlet-oxygen-like species and superoxide radicals. The involvement of hydroxyl radicals in the mechanism pathway of the cleavage mediated by complex **C1** or **C2** suggests that the mode of action of these componds involves mechanisms other than that proposed by Sigman for the copper-phenantroline compound.[35] For two complexes, as in other related compounds with nuclease activity, either a Fenton-type reaction or a Haber-Weiss reaction leads to the formation of oxygen active species which then cleave the DNA.[36]

The ligands have two important roles in the nuclease activity of the complexes: they influence the reactivity of the Cu(II) metal and interact with DNA. The synthesized sulfonamides used as ligands in the Cu(II) complexes increase the reactivity of the metallic ion and the nuclease activity of the complex as compared to simple Cu(II) salts. The presence of aromatic rings like benzene or toluene in the structure of the sulfonamides is probably the main variable determining their capacity to destroy DNA. The complexes have a higher capacity to destroy DNA than the sulfonamide ligand. The planar aromatic rings allow the complex molecule to come closer to DNA through intercalation between neighboring base pairs of the DNA chains, and then link with them through π-stacking bonds. The complex interacts with the DNA molecule (through intercalation in the structure of the double helix). Immediately before or after, the Cu(II) ion is reduced to Cu(I), and, in the presence of molecular oxygen, the formed Cu(I) complex produces reactive oxygen species in close proximity to the double helix. These species finally attack the 2-deoxyribose moiety, leading to the cleavage of the DNA chain.

Bocarsly *et al.*,[37,38] have sugested a mechanism involving hydroxyl radicals, generated by a variety of chemical and physical pathways related to either Fenton or Haber-Weiss reaction:

Fenton mechanism:

$$Cu^{2+}L + AscH^- \rightarrow Cu^{+}L + Asc^{\cdot-} + H^+$$

$$Cu^{+}L + H_2O_2 \rightarrow Cu^{2+}L + OH^- + \cdot OH$$

Haber-Weiss reaction:

$$Cu^{+}L + O_2 \rightarrow Cu^{2+}L + O_2^{\cdot-}$$

$$O_2^{\cdot-} + H_2O_2 \rightarrow {}^1O_2 + HO^- + HO^{\cdot}$$

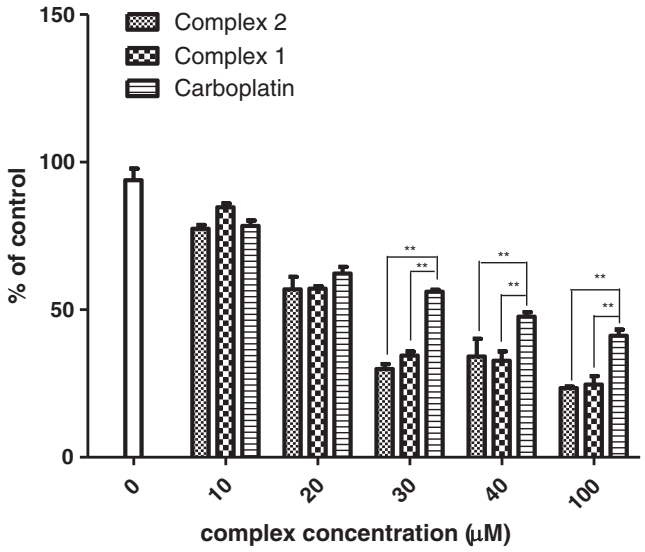

Figure 7. Comparative cytotoxicities of the complex **C1**, complex **C2** and carboplatin on WM35 cultures after 24 hours of exposure at a dose from 10 to 100 μM (versus untreated cells) (mean ± SEM)(n=3)(**=p<0.01).

3.4 *Cytotoxicity of the complexes against WM35 cells*

Complexes **C1** and **C2** were examined for their antiproliferative properties. To analyze this effect of Cu(II) complexes on melanoma cell proliferation we measured the conversion of the water soluble MTT by WM35 cells, using five concentrations ranging between 10 and 100 μM. The inhibitions were compared to those of control (carboplatin). We found a significant inhibition starting at 30 μM, but the higher doses were not more effective, thus a concentration dependent effect could not be established.

Cells were exposed to various concentrations of each compond for 24 h. Figure 7 shows the dose-response graphics for these compounds in terms of the effect of the compound on the growth of the cellular line.

Interpolation of the data points was used to determine the concentration of the complex required to achieve 50% cell death (IC_{50}), with a low IC_{50} implying high cytotoxicity. The IC_{50} values of complexes **C1** and **C2** for the inhibition of cell growth are given in table 4.

Table 4. IC_{50} values of complexes **C1** and **C2** against WM35 cells.

Cells	Complex	IC_{50}(μM)/24 h
WM35 cells	**C1**	23.53 ± 0.23
	C2	21.76 ± 0.34
	Carboplatin	46.23 ± 0.25

*Data represent the mean ± SD of experiments carried out in triplicate

The lowest IC_{50} values were measured for **C2**, indicating a higher cytotoxicity for this complex. According to the IC_{50} data, the two complexes have shown significant inhibition on WM35 cell line. Their activity is better than that of the platinum drug, carboplatin, which was used as control. Statistical analysis showed no significant difference between the two complexes in study, because they have similar structures.

The free ligands showed no significant growth inhibition activity. This indicates that the chelation of ligands $L1^-$ and $L2^-$ with Cu(II) ion is essential for the anticancer activities of these two new complexes.

The results of the cell cytotoxicity are in concordance with the DNA cleavage study and indicate that both complexes have a good antitumor activity. In this study we demonstrated that the complexes have a superior activity comparative with carboplatin and in the future, we will perform *in vivo* studies.

4. Conclusions

A new N-sulfonamide ligand \were synthesized and characterized. The crystalline structures of complexes were determined using X-ray diffraction and were confirmed by the data obtained from elemental analysis, spectral (IR, UV-Vis, EPR) and magnetic determinations. The complexes have a superior nuclease activity as compared to the non-coordinated Cu(II) ion. The use of scavengers of ROS indicates that the hydroxyl, singlet-oxygen species and the superoxide anions are the main radicals that break the DNA strands. The *in vitro* cytotoxicity of the complexes on a carcinoma cell line, WM35 was evaluated. An excellent inhibition of proliferation of cancer cells was exhibited by the two compounds.

Supplementary Information (SI)

Supplementary material has been deposited with the Cambridge Crystallographic Data Centre (nos. 1408834 (**C1**), 1410246 (**C2**) and available free of charge: deposit@ccdc.cam.ac.uk or http://www.ccdc.cam.ac.uk). All additional information pertaining to characterization of the complexes, namely, ^{1}H-NMR, IR spectra. UV-Vis spectra, and EPR spectra (figures S1–S9) are available at www.ias.ac.in/chemsci.

Acknowledgements

Adriana Hangan is thankful for the financial support offered by research grant Resurse Umane PNII -PD 474/2010.

References

1. Sorenson J R J 1992 *Free Rad. Biol. Med.* **13** 593
2. Sorenson J R J 1989 *Prog. Med. Chem.* **26** 437
3. Farrell N 1989 In *Transition Metal Complexes as Drugs and Chemotherapeutic Agents* (Dordrecht: Kluwer Academic) p. 143
4. Garcia-Giménez J L, González-Álvarez M and Liu-González M J 2009 *Inorg. Biochem.* **103** 923
5. Lopez T, Ortiz-Islas E, Guevara P and Gómez E 2013 *Int. J. Nanomed.* **8** 581
6. Zuo J, Bi C, Fan Y, Buac D, Nardon C, Daniel K G and Dou Q P 2013 *J. Inorg. Biochem.* **118** 83
7. Beckford F A, Thessing J, Stott A, Holder A A, Poluektov O G, Li L and Seeram N P 2012 *Inorg. Chem. Commun.* **15** 225
8. Buac D, Schmitt S, Ventro G, Kona F R and Dou Q P 2012 *Mini Rev. Med. Chem.* **12** 1193
9. Anjomshoa M and Torkzadeh-Mahani M 2015 *Spectrochim. Acta, Part A* **150** 390
10. Yousuf I, Arjmand F, Tabassum S, Toupet L, Khan R A and Siddiqui M A 2015 *Dalton Trans.* **44** 10330
11. Ma T, Xu J, Wang Y, Yu H, Yang Y, Liu Y, Ding W, Zhu W, Chen R, Ge Z, Tan Y, Jia L and Zhu T 2015 *J. Inorg. Biochem.* **144** 38
12. Qi J, Liang S, Gou Y, Zhang Z, Zhou Z, Yang F and Liang H 2015 *Eur. J. Med. Chem.* **96** 360
13. Kheirolomoom A, Mahakian L M, Lai C Y, Lindfors H A, Seo J W, Paoli E E, Watson K D, Haynam E M, Ingham E S, Xing L, Cheng R H, Borowsky A D, Cardiff R D and Ferrara K W 2010 *Mol. Pharm.* **7** 1948
14. Owa T, Yoshino H, Okauchi T, Yoshimatsu K, Ozawa Y, Sugi N H, Nagasu T, Koyanagi N and Kitoh K 1999 *J. Med. Chem.* **42** 3789
15. Hangan A C, Turza A, Stan R L, Stefan R and Oprean L S 2015 *Russ. J. Coord. Chem.* **41** 365
16. Hangan A, Bodoki A, Oprean L, Alzuet G, Liu-Gonzalez M and Borras J 2010 *Polyhedron* **29** 1305
17. Bodoki A, Hangan A, Oprean L, Borras J, Castineiras A and Bojiţă M 2008 *Farmacia* **LVI** 607
18. Hangan A, Bodoki A, Oprean L, Crişan O and Mihalca I 2012 *Farmacia* **LV** 932
19. Dolomanov O V, Bourhis L J, Gildea R J, Howard J A K and Puschmann H 2009 *J. Appl. Cryst.* **42** 339
20. Palatinul L and Capuis G 2007 *J. Appl. Cryst.* **40** 786
21. Sheldrick G M (ShelXL) 2008 *Acta Cryst* **A64** 112
22. Gonzalez-Alvarez M, Alzuet G, Borras J, Marcia B and Montejo-Bernardo J M 2003 *Z. Anorg. Allg. Chem.* **23** 15
23. Gutierez L, Alzuet G, Borras J, Liu-Gonzalez M, Sanz F and Castineiras A 2001 *Polyhedron* **20** 703
24. Macias B, Villa M V, Gomez B, Borras J, Alzuet G, Gonzalez-Alvarez M and Castineiras A 2007 *J. Bioinorg. Chem.* **101** 441
25. Allen A M, Kennard O and Watson D G 1987 *Trans. Perkin.* **2** S1
26. Desiraju G R 2003 In *Crystal Design Structure and Function Perspectives in Supramolecular Chemistry* (Chichester: John Wiley) p. 160
27. Koon N, Wong S and Colson D 1984 *J. Mol. Spectrosc.* **104** 129
28. Thomas A M, Nethaji M and Chakravarty A R 2004 *J. Inorg. Biochem.* **98** 1087
29. Cami G E, del C. Ramirez de Arellano M and Fustero S 2006 *An. Asoc. Quim. Argent.* 941
30. Alzuet G, Ferrer S and Borras 1993 *J. Inorg. Chim. Acta* **203** 257
31. Hathaway B J 1987 In *Comprehensive Coordination Chemistry* (New York: Wilkinson & Gillard) ch. 9
32. WINEPR-*Simfonia 1.25*. 1994-1996 (Bruker Analytik GmbH: Karlsruhe)
33. Bertini I and Drago R 1980 In *ESR and NMR of Paramagnetic Species in Biological and Related Systems* (Dordrecht, Holland: Springer Netherlands, D Reidel Publishing Company)
34. Goodman A and Raynor J B 1970 *Adv. Inorg. Chem. Radiochem.* **13** 135
35. Sigman D S 1986 *Acc. Chem. Res.* **19** 180
36. Drevensenk P, Zupancic T, Pihlar B, Jerala R, Kolitsch U, Plaper A and Turel I 2005 *J. Inorg. Biochem.* **99** 432
37. Demeter C A, Pamatong F V and Bocarsly J R 1996 *Inorg. Chem.* **35** 6292
38. Demeter C A, Pamatong F V and Bocarsly J R 1997 *Inorg. Chem.* **36** 3676